J. Fluid Mech. (1975), *vol.* 67, *part* 4, *pp.* 723–742
Printed in Great Britain

Pendular rings between solids: meniscus properties and capillary force

By F. M. ORR, L. E. SCRIVEN

Department of Chemical Engineering and Materials Science, University of Minnesota, Minneapolis

AND A. P. RIVAS

Facultad de Ingeniería Química, Universidad Pontificia Bolivariana, Medellín, Columbia

(Received 29 March 1974)

The Laplace–Young equation is solved for axisymmetric menisci, analytically in terms of elliptic integrals for all possible types of pendular rings and liquid bridges when the effect of gravity is negligible, numerically for selected other cases in order to assess gravity's effect. Meniscus shapes, mean curvatures, areas and enclosed volumes are reported, as are capillary forces. It is shown that capillary attraction may become capillary repulsion when wetting is imperfect. The special configurations of vanishing capillary force and of zero mean curvature are treated. The range of utility of the convenient 'circle approximation' is evaluated.

1. Introduction

A small amount of liquid held at a point of contact between two solid surfaces is often called a pendular ring if its meniscus is axially symmetric or nearly so. If the surfaces are slightly apart the liquid may form an axially symmetric liquid bridge between them. These ring and bridge configurations occur in a broad range of circumstances and consequently investigators from widely separated fields have attacked various aspects of the problem of describing them. Of importance in applications are the volume of liquid, surface area and mean curvature of the meniscus, and forces exerted on the solid surfaces. For instance, volume is central to calculations of water saturations in soils (Haines 1925; Fisher 1926), assessment of connate water content of oil and gas reservoirs (Morrow 1971), and interpretation of mercury porosimetry data (Mayer & Stowe 1966). Curvature is crucial in calculations of capillary condensation and evaporation in all sorts of porous media (Defay & Prigogine 1966; Everett 1967; Melrose 1972). Forces are important in the dispersion of pigments and wetting of powders (Carman 1953), flocculation of three-phase slurries (Woodrow, Chilton & Hawes 1961), deformation of moist soils and other unconsolidated porous media (Haines 1925, 1927; Fisher 1926), liquid-phase sintering of finely divided metals or polymers (Kingery 1959; Heady & Cahn 1970), formation of latex films (Sheetz

1965; Vanderhoff *et al.* 1966; Mason 1973), and adhesion of dust and powder to surfaces (Zimon 1960).

When the amount of trapped liquid is small enough that the influence of gravity is negligible, the meniscus everywhere has the same mean curvature. To find surfaces of uniform, non-vanishing mean curvature which have prescribed area and enclose a maximum or minimum volume is a classic problem in the calculus of variations and the axisymmetric case was considered by Howe (1887). Using a method similar to Howe's, in which interpolation among solutions is required in order to satisfy boundary conditions, Fisher (1926) calculated the volumes of and forces exerted by pendular rings between identical spheres which are completely wetted by the trapped liquid; in this case the meniscus is a segment of nodoid. Woodrow *et al.* (1961) calculated meniscus profiles and adhesive forces by solving the Laplace–Young differential equation (which is the Euler equation of the equivalent variational problem) as an initial-value problem with the radius of the meniscus given on the plane of symmetry between identical spheres; interpolation among the profiles selects the one which makes the prescribed contact angle with spheres of given size. The corresponding boundary-value problem was solved by Melrose (1966), who obtained volumes, areas and curvatures but limited himself to menisci with negative mean curvatures (a curvature is considered positive when its centre of curvature lies on the axis-side of the meniscus) and consequently missed some interesting features of the solution set. Erle, Dyson & Morrow (1971) studied the stability of liquid bridges and also obtained some but not all members of the solution set. For the problem of a meniscus between spheres of unequal radius only an approximate solution has been attempted (Rose 1958). None of these investigations has dealt with the effect of a different contact angle at each sphere.

In fact there has been no comprehensive analysis of pendular rings and liquid bridges, even of those between identical spheres. In this paper we treat the more general case of a sphere in contact with a flat plate, the meniscus making different contact angles at the sphere and the plate. This subsumes rings and bridges between unequal spheres as well as between equal spheres with different contact angles, inasmuch as solutions to these problems can be constructed from solutions of the sphere-on-plate problem which intersect the plane of the plate in a common circle and make supplementary contact angles with that plane. The system to be treated is shown in figure 1. Approximate solutions were attempted for the sphere-on-plate problems by Cross & Picknett (1963*b*) and Clark, Haynes & Mason (1968).

In the next section the Laplace–Young equation is solved in terms of elliptic integrals for all possible types of pendular rings between sphere and plate when the effect of gravity is negligible. Computations based on these results are reported in §3, which contains new information about rings having zero mean curvature (an instance of 'Plateau's problem') and about rings which produce zero net force on the sphere. The occurrence of capillary repulsion is analysed. Finally a commonly used 'circle approximation' is extended to the more general sphere-on-plate problem and its range of validity is considered.

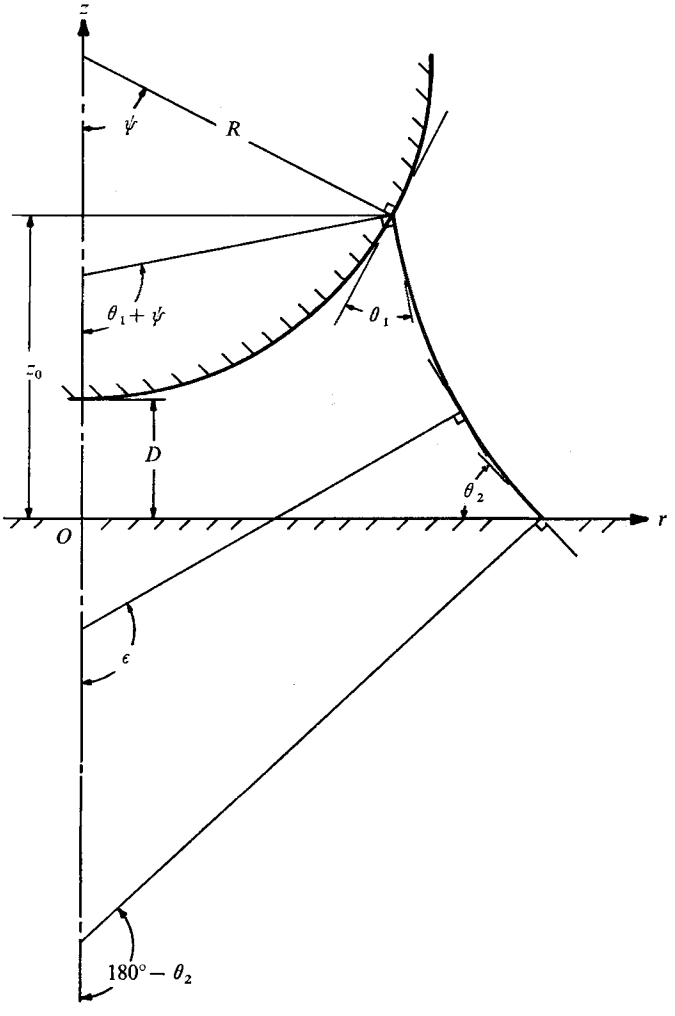

FIGURE 1. Pendular ring or liquid bridge between a sphere and a plane.

2. Analysis

The configuration of a liquid/vapour interface at rest is described by the equation of Young and Laplace (Pujado, Huh & Scriven 1972), which relates the difference in hydrostatic pressure across the interface to the local mean curvature H and surface tension σ of the interface. When the Bond number ($gL^2\Delta\rho/\sigma$, where g is the local acceleration due to gravity, $\Delta\rho$ the density difference between the fluids on either side of the interface, and L some characteristic length for the system) is sufficiently small, the effect of gravity is negligible and the mean curvature is nearly uniform. If the meniscus is axisymmetric its mean curvature then satisfies the following version of the Laplace–Young equation:

$$2H = \frac{d^2z/dr^2}{[1+(dz/dr)^2]^{\frac{3}{2}}} + \frac{dz/dr}{r[1+(dz/dr)^2]^{\frac{1}{2}}}; \tag{1}$$

r and z are cylindrical co-ordinates of the meniscus (figure 1). With dimensionless variables $y = z/R$ and $x = r/R$ and the parameter $u = -\sin\epsilon$ (Melrose 1966), where ϵ is the angle made by the normal to the meniscus with the vertical axis, (1) reduces to

$$2HR = -du/dx - u/x. \tag{2}$$

This equation must be solved as a two-point boundary-value problem for which the boundary conditions are the inclinations of the meniscus at the contact circles where it terminates on solid surfaces. These inclinations are determined by the slopes of the solid surfaces and the respective contact angles θ_1 and θ_2 which the meniscus makes with them. Thus the boundary conditions are

$$\left.\begin{aligned} u_2 &= -\sin(\pi-\theta_2), \quad y_2 = 0, \\ u_1 &= -\sin(\theta_1+\psi), \quad y_1 = d+1-\cos\psi, \quad x_1 = \sin\psi, \end{aligned}\right\} \tag{3}$$

where ψ is the filling angle and $d = D/R$ is the separation between sphere and plate (see figure 1).

The boundary-value problem has the solution

$$x = -(1/2H)\,[u \mp (u^2+c)^{\frac{1}{2}}], \tag{4}$$

$$y = \frac{1}{2HR}\int_{u_2}^{u}\left(\frac{u\,du}{(1-u^2)^{\frac{1}{2}}}\,\frac{u \mp (u^2+c)^{\frac{1}{2}}}{\mp (u^2+c)^{\frac{1}{2}}}\right), \tag{5}$$

where the curvature-dependent parameter c is

$$c \equiv 4H^2R^2\sin^2\psi - 4HR\sin\psi\sin(\theta_1+\psi).$$

The mean curvature can be obtained from (5):

$$2HR = \frac{1}{y_1}\int_{u_2}^{u_1}\left(\frac{u\,du}{(1-u^2)^{\frac{1}{2}}}\,\frac{u \mp (u^2+c)^{\frac{1}{2}}}{\mp (u^2+c)^{\frac{1}{2}}}\right). \tag{6}$$

An iterative solution is required since c depends on H.

The choice between ambiguous signs in (4)–(6) is dictated by the sign of the meridional curvature of the meniscus. In (2) the meridional curvature is $-du/dx$ and the azimuthal curvature $-u/x$. Therefore the meridional curvature can be expressed as

$$-\frac{du}{dx} = \frac{-2Hu}{u \mp (u^2+c)^{\frac{1}{2}}} + 2H. \tag{7}$$

We consider first a meniscus with negative meridional curvature,

$$-du/dx < 0, \tag{8}$$

for which the mean curvature H is either positive or not. We note that x, the dimensionless radius, is necessarily positive, and so from (4) we require that

$$x = -[-\sin\epsilon \pm (\sin^2\epsilon + c)^{\frac{1}{2}}]/2H > 0. \tag{9}$$

If $H \leqslant 0$, then $c \geqslant 0$ and

$$(\sin^2\epsilon + c)^{\frac{1}{2}} \geqslant \sin\epsilon$$

and hence the plus sign must be chosen if (9) is to be satisfied when $H < 0$. Similarly, where $H > 0$ and $c \geqslant 0$, the minus sign must be used.

When $0 < H < \sin(\theta_1+\psi)/\sin\psi$, then $c < 0$. Now let

$$\frac{\sin\epsilon}{-\sin\epsilon \mp (\sin^2\epsilon+c)^{\frac{1}{2}}} \equiv K.$$

If the minus sign is chosen in the definition of K, it follows that $-1 < K < -\frac{1}{2}$ and if the plus sign is chosen, $K < -1$. Consequently (7) becomes

$$-du/dx = 2H(K+1)$$

and the plus sign in (7) must be used if the meridional curvature is negative. Similarly, the minus sign must be used when the meridional curvature is positive. Hence the appropriate sign in (4)–(6) is the opposite of the sign of the meridional curvature.

In some instances the meridional curvature changes sign at an intermediate point, an inflexion point, in the meridional profile. At such a point the meridional curvature $-du/dx$ is zero and (2) becomes

$$2H = -\frac{u}{x} = \frac{u}{(2H)^{-1}[u \mp (u^2+c)^{\frac{1}{2}}]}$$

or $u \mp (u^2+c)^{\frac{1}{2}} = u$; i.e. at an inflexion point

$$u^2+c = 0. \tag{10}$$

Hence c must be negative, which requires that

$$0 < HR < \sin(\theta_1+\psi)/\sin\psi. \tag{11}$$

In terms of the parameter ϵ, which is the angle between the normal to the meniscus and the vertical axis, the inflexion point occurs at

$$\epsilon^* = \arcsin(-c)^{\frac{1}{2}}.$$

If an inflexion point does occur in the meridional profile, then a singularity appears in the integral in (5) and (6), which consequently must be broken up into parts, each with the appropriate choice of signs. There might be more than one inflexion point yet no more than one was found with any of the pairs of contact angles for which computations were made (all for zero separation between sphere and plane). Multiple inflexions in the meridional profiles of other solutions of (2) are known (Plateau 1864) but such menisci are likely to be unstable.

When $0 < \theta_1+\theta_2 < \pi$ and $\theta_2 \neq \frac{1}{2}\pi$ and $\theta_2 \neq 0$, an inflexion point appears as the filling angle ψ increases. From (10) we can predict the mean curvatures at which an inflexion point occurs at either the plate or the sphere. At the sphere, $\epsilon_1 = \theta_1+\psi$ and (10) becomes

$$H_s^* = \sin(\theta_1+\psi)/2\sin\psi. \tag{12}$$

At the plate, $\epsilon_2 = \pi-\theta_2$ and (10) becomes

$$H_p^* = \{\sin(\theta_1+\psi) \mp [\sin^2(\theta_1+\psi) - \sin^2(\pi-\theta_2)]^{\frac{1}{2}}\}/2\sin\psi. \tag{13}$$

Because the mean curvature H is of course a function of the filling angle ψ, computations with (12) and (13) must rely on some iterative process to arrive at precise values of H and ψ. We note that (13) has one root such that $H_p^* < H_s^*$ and another such that $H_p^* > H_s^*$. Numerical computations for specific values of θ_1 and θ_2 have shown that, when $\theta_2 < \frac{1}{2}\pi$, the minus sign applies and the second apparent root of (13) is not admissible since $\sin^2(\theta_1+\psi) < \sin^2(\pi-\theta_2)$. Similarly, when $\theta_2 > \frac{1}{2}\pi$, the plus sign is appropriate and the other root is not admissible. Computations have also shown that the slope of $H(\psi)$ is positive in the range of ψ where inflexion points occur, so that with increasing ψ the inflexion point appears at the sphere if $H_s^* < H_p^*$ and at the plate if $H_s^* > H_p^*$. In either event, as ψ increases further the point then migrates along the profile until it reaches the other end.

When both θ_1 and θ_2 are small, there is an inflexion point in every profile over a large range of filling angles ψ (cf. figure 3). As θ_2 increases, the range narrows and at $\theta_2 = \frac{1}{2}\pi$ it collapses to a single profile for which $\theta_2+\psi = \frac{1}{2}\pi$: the meniscus is a right cylinder. When $\theta_1+\theta_2 \geqslant \pi$, the mean curvature falls outside the range given by (11) regardless of ψ. At $\theta_2 = 0$, the range again collapses to a single point, but the solution is degenerate in the sense that the radius of the meniscus at the plate becomes infinite. Otherwise there is always a range of filling angles ψ between the values for the zero-curvature and zero-force configurations (see § 3) in which the meniscus profile contains an inflexion point, a fact not heretofore noted.

On the presumption that no more than one inflexion point occurs in the meridional profile, (5) and (6) can be rewritten in terms of elliptic integrals F and E of the first and second kinds. The exact form of (5) and (6) and of related equations for the meniscus surface area and volume enclosed by meniscus of course depends on the sign of the meridional curvature and whether or not there is an inflexion point at which it changes sign, causing singularities to appear in the integrals. All of the formulae for the mean curvature, meridional profile, surface area and enclosed volume have been worked out and are summarized in tables 1–3. The various forms are merely different versions of the same solution and each can be obtained from others by appropriately transforming elliptic integrals or taking limits. The results tabulated here reduce to those obtained by Woodrow *et al.* (1961) and Melrose (1966) for the case $\theta_2 = \frac{1}{2}\pi$, in which the plane can be regarded as the plane of symmetry between identical spheres.

3. Discussion

Plateau's sequence

As the filling angle is increased, the profiles generated with the formulae in tables 1 and 2 follow the sequence of surfaces of constant mean curvature classified by Plateau (1864), although for certain ranges of contact angles θ_1 and θ_2, the succession begins or ends in the middle of the full sequence. Examples are shown in figure 2. At first the meniscus is a portion of nodoid having sufficiently negative meridional curvature that the mean curvature is negative and the pressure inside the meniscus is lower than that of the surroundings.

Surface description	Meridional curvature at sphere	Dimensionless mean curvature, $2HR$	Range and conditions
Nodoid	< 0	$\Psi\left\{\Theta - \frac{1}{k}[E(\phi_2,k) - E(\phi_1,k)] + \frac{1-k^2}{k}[F(\phi_2,k) - F(\phi_1,k)]\right\}$	$H < 0$
Catenoid	< 0	0	$H = 0$
Unduloid (no inflexion)	< 0	$\Psi\{\Theta + E(\alpha_1,k_1) - E(\alpha_2,k_1)\}$	$\theta_2 \lesseqgtr \frac{1}{2}\pi$ $0 < H < \sin(\theta_1+\psi)/\sin\psi$
Unduloid (with inflexion)	$\lesseqgtr 0$	$\Psi\{\Theta + 2E(k_1) \pm E(\alpha_1,k_1) \pm E(\alpha_2,k_1)\}$ $\Psi\{\Theta + 2E(k_1) - E(\alpha_1,k_1) - E(\alpha_2,k_1)\}$	
Unduloid (no inflexion)	> 0	$\Psi\{\Theta - E(\alpha_1,k_1) + E(\alpha_2,k_1)\}$	
Sphere	> 0	$\Psi\Theta + \sin(\theta_1+\psi)/\sin\psi = 2\sin(\theta_1+\psi)/\sin\psi$	$H = \sin(\theta_1+\psi)/\sin\psi$
Nodoid	> 0	$\Psi\left\{\Theta + \frac{1}{k}[E(\phi_2,k) - E(\phi_1,k)] - \frac{1-k^2}{k}[F(\phi_2,k) - F(\phi_1,k)]\right\}$	$H > \sin(\theta_1+\psi)/\sin\psi$

$\Psi \equiv 1/(d+1-\cos\psi)$ $\quad \phi_1 = -(\theta_1+\psi)+\frac{1}{2}\pi$ $\quad \alpha_1 \equiv \arcsin(k\sin\phi_1)$ $\quad k \equiv 1/(1+c)^{\frac{1}{2}}$ (c defined in the text)

$\Theta \equiv -\cos(\theta_1+\psi) - \cos\theta_2$ $\quad \phi_2 \equiv \theta_2 - \frac{1}{2}\pi$ $\quad \alpha_2 \equiv \arcsin(k\sin\phi_2)$ $\quad k_1 \equiv 1/k$

TABLE 1. Mean curvature of pendular-ring and liquid-bridge forms between sphere and plane

Surface description	Meridional curvature	Dimensionless radius, $x = r/R$	Dimensionless height, $y = z/R$	
Nodoid	< 0	$\frac{1}{2HR}[\sin\epsilon - (\sin^2\epsilon + c)^{\frac{1}{2}}]$	$\frac{1}{2HR}\left\{-\cos\epsilon - \cos\theta_2 - \frac{1}{k}[E(\phi_2, k) - E(\phi, k)] + \frac{1-k^2}{k}[F(\phi_2, k) - F(\phi, k)]\right\}$	
Catenoid	< 0	$\sin\psi \sin(\theta_1 + \psi)/\sin\epsilon$	$-\sin\psi \sin(\theta_1 + \psi) \ln[\tan(\frac{1}{2}\epsilon)\tan(\frac{1}{2}\theta_2)]$	
Unduloid (no inflexion)	< 0	$\frac{1}{2HR}[\sin\epsilon - (\sin^2\epsilon + c)^{\frac{1}{2}}]$	$\frac{1}{\Psi} - \frac{1}{2HR}\{-\cos(\theta_1 + \psi) + \cos\epsilon - E(\alpha, k_1) + E(\alpha_1, k_1)\}$	
Unduloid (with inflexion)	< 0 at sphere	$\frac{1}{2HR}[\sin\epsilon - (\sin^2\epsilon + c)^{\frac{1}{2}}]$	$\frac{1}{\Psi} - \frac{1}{2HR}\{-\cos(\theta_1 + \psi) + \cos\epsilon - E(\alpha, k_1) + E(\alpha_1, k_1)\}$,	$\frac{1}{\Psi} > y > y^*$
	> 0 at plane	$\frac{1}{2HR}[\sin\epsilon + (\sin^2\epsilon + c)^{\frac{1}{2}}]$	$y^* - \frac{1}{2HR}\{-\cos\epsilon^* + \cos\epsilon + E(k_1) + E(\alpha, k_1)\}$,	$0 < y < y^*$
Unduloid (with inflexion)	> 0 at sphere	$\frac{1}{2HR}[\sin\epsilon + (\sin^2\epsilon + c)^{\frac{1}{2}}]$	$\frac{1}{\Psi} - \frac{1}{2HR}\{-\cos(\theta_1 + \psi) + \cos\epsilon + E(\alpha, k_1) - E(\alpha_1, k_1)\}$,	$\frac{1}{\Psi} > y > y_*$
	< 0 at plane	$\frac{1}{2HR}[\sin\epsilon - (\sin^2\epsilon + c)^{\frac{1}{2}}]$	$y_* - \frac{1}{2HR}\{-\cos\epsilon^* + \cos\epsilon + E(k_1) - E(\alpha, k_1)\}$,	$0 < y < y_*$
Unduloid (no inflexion)	> 0	$\frac{1}{2HR}[\sin\epsilon + (\sin^2\epsilon + c)^{\frac{1}{2}}]$	$\frac{1}{\Psi} - \frac{1}{2HR}\{-\cos(\theta_1 + \psi) + \cos\epsilon + E(\alpha, k_1) - E(\alpha_1, k_1)\}$	
Sphere	> 0	$\sin\psi + \frac{1}{\Psi\Theta}[\sin\epsilon - \sin(\theta_1 + \psi)]$	$\frac{1}{\Psi} + \frac{1}{\Psi\Theta}[\cos(\theta_1 + \psi) - \cos\epsilon]$	
Nodoid	> 0	$\frac{1}{2HR}[\sin\epsilon + (\sin^2\epsilon + c)^{\frac{1}{2}}]$	$\frac{1}{2HR}\left\{-\cos\epsilon - \cos\theta_2 + \frac{1}{k}[E(\phi_2, k) - E(\phi, k)] - \frac{1-k^2}{k}[F(\phi_2, k) - F(\phi, k)]\right\}$	

$\phi = \frac{1}{2}\pi - \epsilon$ $\quad y^* = \frac{1}{\Psi} - \frac{1}{2HR}[-\cos(\theta_1 + \psi) + \cos\epsilon^* + E(k_1) + E(\alpha_1, k_1)]$

$\alpha = \arcsin(k\sin\phi)$

$\epsilon^* = \arcsin(-c)^{\frac{1}{2}}$ $\quad y_* = \frac{1}{\Psi} - \frac{1}{2HR}[-\cos(\theta_1 + \psi) + \cos\epsilon^* + E(k_1) - E(\alpha_1, k_1)]$

} Height of inflexion point

TABLE 2. Meniscus profiles of pendular-ring and liquid-bridge forms between sphere and plane

Surface description	Dimensionless area of surface of revolution, A/R^2	Dimensionless volume of surface of revolution,† V/R^3
Nodoid	$\delta+\frac{\pi kc}{2H^2}[F(\phi_1,k)-F(\phi_2,k)]$	$\omega\{\mu+\nu+\eta-\frac{1}{3}kc(c+4)[F(\phi_1,k)-F(\phi_2,k)]+\frac{1}{3}k(c+8)(c+1)[E(\phi_1,k)-E(\phi_2,k)]\}$
Catenoid	$2\pi\sin^2\psi\sin^2(\theta_1+\psi)\left\{\frac{\cos\theta_2}{2\sin^2\theta_2}-\frac{\cos(\theta_1+\psi)}{2\sin^2(\theta_1+\psi)}+\frac{1}{2}\ln\left\lvert\frac{\tan[\frac{1}{2}(\theta_1+\psi)]}{\tan[\frac{1}{2}(\pi-\theta_2)]}\right\rvert\right\}$	$\pi\sin^3\psi\sin^3(\theta_1+\psi)\left\{\frac{\cos\theta_2}{2\sin^2\theta_2}-\frac{\cos(\theta_1+\psi)}{2\sin^2(\theta_1+\psi)}+\frac{1}{2}\ln\left\lvert\frac{\tan[\frac{1}{2}(\theta_1+\psi)]}{\tan[\frac{1}{2}(\pi-\theta_2)]}\right\rvert\right\}$
Unduloid (no inflexion)	$\delta+(\pi c/2H^2)[F(\alpha_1,k_1)-F(\alpha_2,k_1)]$	$\omega\{\mu+\nu+\eta+\frac{4}{3}c[F(\alpha_1,k_1)-F(\alpha_2,k_1)]+\frac{1}{3}(c+8)[E(\alpha_1,k_1)-E(\alpha_2,k_1)]\}$
Unduloid (with inflexion)	$\delta+(\pi c/2H^2)[2F(k_1)+F(\alpha_1,k_1)+F(\alpha_2,k_1)]$	$\omega\{\mu+\nu-\eta+\frac{4}{3}c[2F(k_1)+F(\alpha_1,k_1)+F(\alpha_2,k_1)]+\frac{1}{3}(c+8)[2E(k_1)+E(\alpha_1,k_1)+E(\alpha_2,k_1)]\}$
	$\delta+(\pi c/2H^2)[2F(k_1)-F(\alpha_1,k_1)-F(\alpha_2,k_1)]$	$\omega\{\mu-\nu+\eta+\frac{4}{3}c[2F(k_1)-F(\alpha_1,k_1)-F(\alpha_2,k_1)]+\frac{1}{3}(c+8)[2E(k_1)-E(\alpha_1,k_1)-E(\alpha_2,k_1)]\}$
Unduloid (no inflexion)	$\delta-(\pi c/2H^2)[F(\alpha_1,k_1)-F(\alpha_2,k_1)]$	$\omega\{\mu-\nu-\eta-\frac{4}{3}c[F(\alpha_1,k_1)-F(\alpha_2,k_1)]-\frac{1}{3}(c+8)[E(\alpha_1,k_1)-E(\alpha_2,k_1)]\}$
Sphere	$2\pi\beta[\tau(\psi+\theta_1+\theta_2-\pi)+\beta\Theta]$	$\pi\beta\{\Theta[\tau^2+\beta^2]+\frac{1}{3}\beta^3[\cos^3(\theta_1+\psi)+\cos^3\theta_2]+\beta\tau[\psi+\theta_1+\theta_2-\pi-\frac{1}{2}\sin(2\theta_1+2\psi)-\frac{1}{2}\sin(2\theta_2)]\}$
Nodoid	$\delta-(\pi kc/2H^2)[F(\phi_1,k)-F(\phi_2,k)]$	$\omega\{\mu-\nu-\eta+\frac{1}{3}kc(c+4)[F(\phi_1,k)-F(\phi_2,k)]-\frac{1}{3}k(c+8)(c+1)[E(\phi_1,k)-E(\phi_2,k)]\}$

$\delta\equiv 2\pi/HR\Psi$ $\quad\omega\equiv\pi/(2HR)^3$ $\quad\mu\equiv(c+4)\Theta+\frac{4}{3}[\cos^3(\theta_1+\psi)+\cos^3\theta_2]$

$\beta=\dfrac{1}{\Psi\Theta}$ $\quad\tau=\sin\psi-\beta\sin(\theta_1+\psi)$ $\quad\nu=\frac{4}{3}\sin(\theta_1+\psi)\cos(\theta_1+\psi)[\sin^2(\theta_1+\psi)+c]^{\frac{1}{2}}$

$\eta=\frac{4}{3}\sin\theta_2\cos\theta_2(\sin^2\theta_2+c)^{\frac{1}{2}}$

† Subtract volume of wetted spherical segment $\pi(\frac{2}{3}-\cos\psi+\frac{1}{3}\cos^3\psi)$ to obtain ring volume. See table 1 for ranges and other definitions.

TABLE 3. Surface area and volume of pendular-ring and liquid-bridge forms between sphere and plane

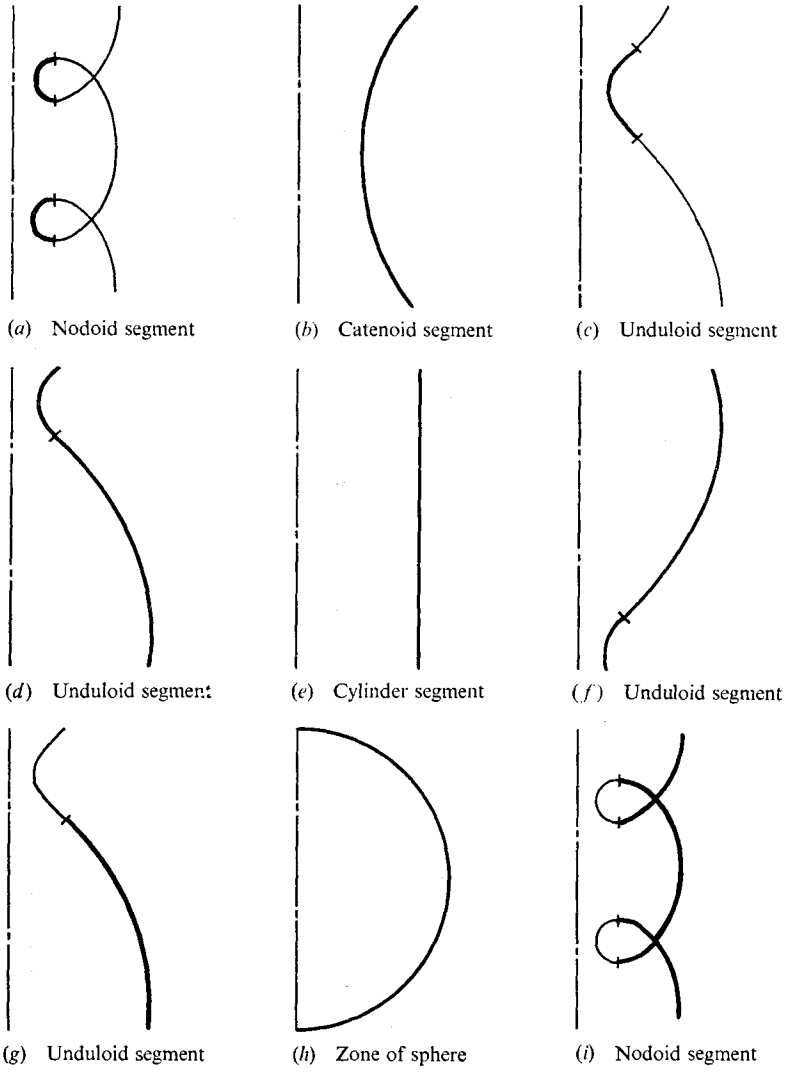

FIGURE 2. Classification by profiles of axisymmetric menisci of uniform mean curvature. Meridional curvatures: (*a*)–(*c*) negative; (*d*) negative at sphere and positive at plane; (*e*) everywhere zero; (*f*) positive at sphere and negative at plane; (*g*)–(*i*) everywhere positive. Except in (*a*) and (*i*), tick marks indicate inflexion points.

With increasing filling angle ψ the surface eventually becomes a catenoid having zero mean curvature; the pressure inside the meniscus equals that outside. With further increase in ψ, the meniscus becomes a portion of unduloid having negative meridional curvature but positive mean curvature. At all larger filling angles the mean curvature remains positive and the pressure inside the meniscus is higher than outside. As we have established, an inflexion point appears sooner or later (if $\theta_2 \neq 0$) either at the plate or at the sphere, and migrates with increasing ψ along the profile, which is still the profile of a portion of unduloid. When the inflexion point leaves the profile, the meniscus becomes a portion of

Filling angle, ψ (deg)	Mean curvature $2HR$		Net force on sphere $F_t/\pi R\sigma$		Volume of ring V/R^3		Surface area of ring A/R^2		Meniscus radius at plane, r/R	
	$\theta_1 = \theta_2 = 0$	$\theta_1 = \theta_2 = 40°$	$\theta_1 = \theta_2 = \theta$	$\theta_1 = \theta_2 = 40°$	$\theta_1 = \theta_2 = 0$	$\theta_1 = \theta_2 = 40°$	$\theta_1 = \theta_2 = 0$	$\theta_1 = \theta_2 = 40°$	$\theta_1 = \theta_2 = 0$	$\theta_1 = \theta_2 = 40°$
10	−125·965	−87·4644	3·8586	2·9034	0·0006	0·0007	0·0244	0·0183	0·1750	0·1750
20	−29·7128	−18·2938	3·7097	2·7324	0·0091	0·0107	0·1826	0·1424	0·3533	0·3529
30	−12·2150	−6·4447	3·5538	2·5509	0·0421	0·0527	0·5837	0·4699	0·5394	0·5373
40	−6·2055	−2·6435	3·3903	2·3583	0·1237	0·1650	1·3295	1·0990	0·7391	0·7321
50	−3·4836	−1·0589	3.2179	2·1535	0·2878	0·4063	2·5433	2·1415	0·9611	0·9429
60	−2·0459	−0·3061	3·0344	1·9353	0·5856	0·8668	4·4152	3·7411	1·2179	1·1761
70	−1·2129	0·0721	2·8371	1·7024	1·1021	1·6909	7·2925	6·1025	1·5294	1·4406
80	−0·7040	0·2596	2·6225	1·4540	1·9954	3·1202	11·8875	9·5351	1·9301	1·7478
90	−0·3867	0·3419	2·3867	−1·1902	3·5954	5·5741	19·8379	14·5205	2·4843	2·1123
100	−0·1920	0·3635	2·1259	−0·9135	6·7005	9·7918	35·4953	21·7959	3·3279	2·5517
110	−0·0799	0·3507	1·8366	0·6300	13·6708	17·0453	73·1049	32·4140	4·7938	3·0832
120	−0·0243	0·3205	1·5183	0·3520	33·9432	29·3208	197·041	47·6282	7·8988	3·7151
130	−0·0041	0·2850	1·1760	0·0988	130·239	49·0300	911·379	68·3126	17·0227	4·4319
140	−0·0002	0·2523	0·8264	−0·1042	1461·99	77·3541	14190·7	93·6766	67·2069	5·1756
150		0·2270		−0·2304		110·745		119·673		5·8375
160		0·2118		−0·2587		137·622		138·384		6·2655
170		0·2094		−0·1800		139·802		139·362		6·2753

TABLE 4. Properties of pendular rings between sphere and plane when $\theta_1 = \theta_2 = 40°$

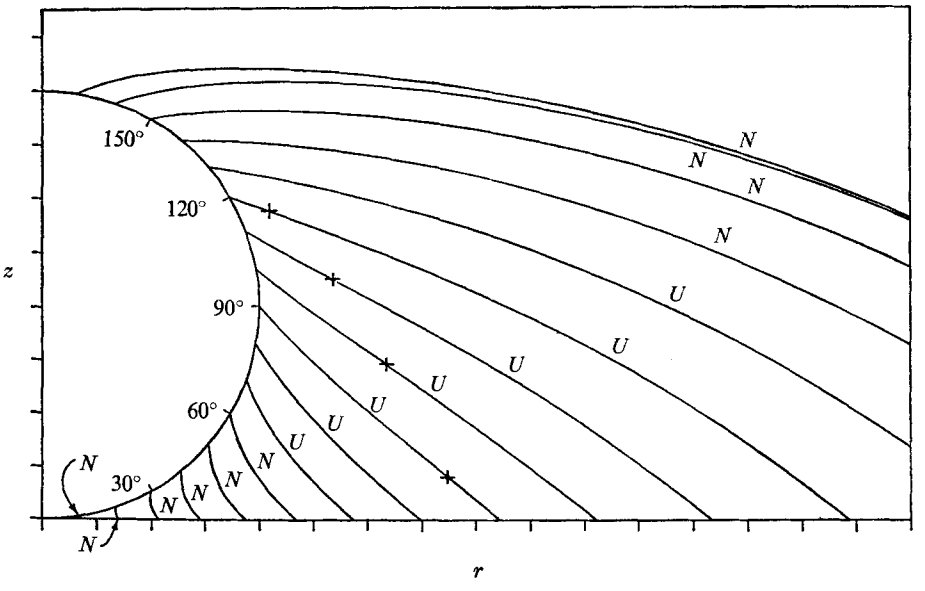

FIGURE 3. Meniscus profiles when $\theta_1 = 40°$ and $\theta_2 = 40°$, i.e. imperfect wetting. +, inflexion points; N, nodoid; U, unduloid.

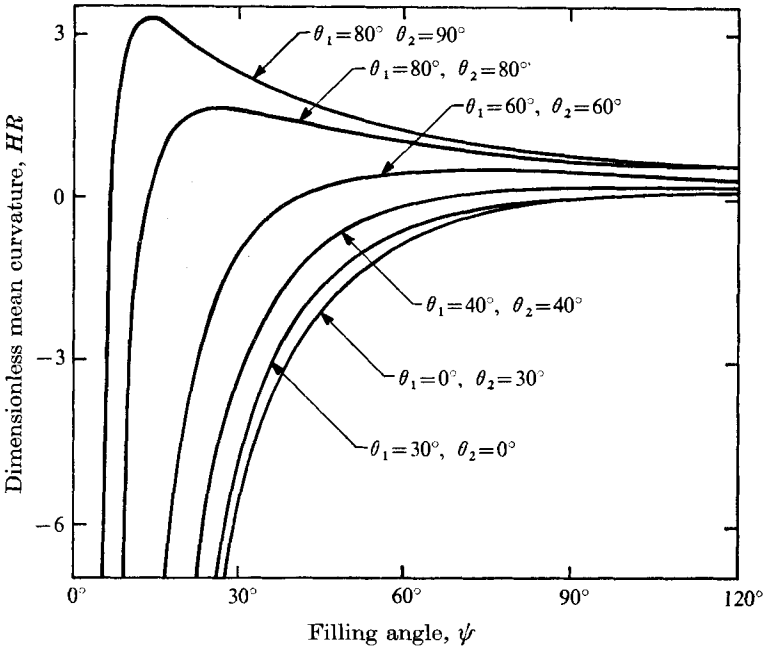

FIGURE 4. Mean curvature of meniscus *vs.* filling angle of pendular ring (sphere on plate) for assorted contact-angle pairs.

unduloid having positive meridional curvature. Eventually the meniscus becomes a portion of sphere and finally a portion of nodoid again but with positive meridional and mean curvatures.

Figure 3 shows profiles computed using the formulae in table 2 for a sphere in contact with the plate and contact angles of 40° on both. Inflexion points are marked by a + on curves where they occur and can be seen to proceed from the plate to the sphere as ψ increases. The mean curvature, net force, volume, surface area and meniscus radius at the plate for the same case as well as the experimentally important case of zero contact angles on both the sphere and plate are shown in table 4.

Meniscus curvature

Results of computations using the formulae listed in table 1 for zero separation between sphere and plate and a variety of contact-angle pairs are shown in figure 4. Where $\theta_2 \neq 0$ the mean curvature has a relative maximum with respect to the filling angle ψ and in some circumstances it also has a relative minimum. At both the maximum and the minimum the mean curvature is positive. When there is a minimum it occurs at a larger filling angle than the maximum. Thus there are values of H which could exist at as many as three different filling angles. Because the curvature of the meniscus affects the vapour pressure of liquid inside the meniscus, as described by the Kelvin equation (Defay & Prigogine 1966), the value of H determines whether liquid inside the meniscus is in diffusional equilibrium with vapour at a particular pressure. As the Kelvin equation teaches (see appendix), when $H < 0$ equilibrium is possible between a pendular ring or bridge of liquid and vapour at a certain pressure less than the ordinary vapour pressure (pressure of vapour in equilibrium with liquid at the same temperature behind a flat meniscus). Moreover, it is easy to see that the equilibrium is stable with respect to small perturbations of liquid volume by vaporization or condensation (see appendix). Thus when the mean curvature is negative there is a single equilibrium state (ψ, H) and it is stable with respect to isothermal diffusional equilibrium. On the other hand, when the mean curvature is positive, $H > 0$, equilibrium is possible only with vapour at a certain pressure above the ordinary vapour pressure. While there may be as many as three equilibrium filling angles, it is not hard to see that no more than one can be stable to small perturbations of liquid volume by vaporization or condensation (see appendix).

The catenoid, a surface of zero mean curvature, has special significance because it is the shape which can exist in diffusional equilibrium with vapour which is also in equilibrium with bulk liquid at the same temperature. According to the appropriate form of (5) – catenoid entry in table 1 – and the boundary condition at the sphere, the catenoid occurs when ψ satisfies

$$\tan\left(\frac{\theta_1+\psi_c}{2}\right)\exp\left\{\frac{\tan\left(\frac{1}{2}\psi_c\right)}{\sin\left(\theta_1+\psi_c\right)}\right\} = \cot\left(\frac{\theta_2}{2}\right). \tag{14}$$

Figure 5 is a plot of the filling angles ψ_c at which the mean curvature of menisci between a sphere and plate in contact vanishes when the contact angles are

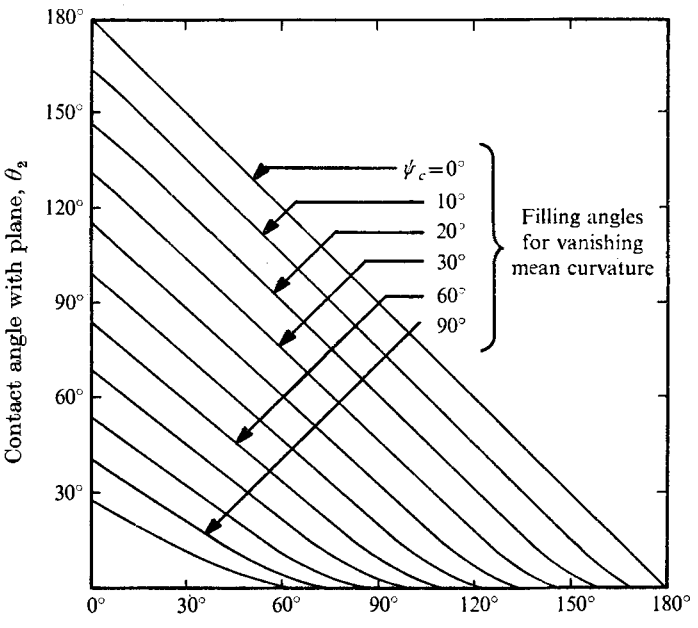

FIGURE 5. Filling angles for vanishing mean curvature of pendular ring (sphere on plate). Above the diagonal the mean curvature is always positive (pressure greater inside than outside the ring); below the diagonal the mean curvature is negative if $\psi < \psi_c$, i.e. if the filling angle is less than the angle given by the curve through the point (θ_1, θ_2).

θ_1 and θ_2. Plainly, if $\theta_2 = 0$, equation (14) is satisfied only by $\theta_1 + \psi = \pi$ and this corresponds to a meniscus of unbounded radius at the plate. Except for this unlikely case the mean curvature is necessarily negative when liquid wets the plate perfectly, i.e. when $\theta_2 = 0$. When the sphere is perfectly wet, $\theta_1 = 0$, and the configuration of zero mean curvature occurs at some $\psi_c < 180°$. In general, as wetting deteriorates, i.e. as θ_1 and θ_2 increase, the catenoid occurs at lower ψ_c.

Capillary force

The total force exerted through ring or bridge on the sphere and the plate consists of three parts: a surface-tension force which resides in the meniscus, a capillary pressure force which is transmitted by the liquid but originates in the curvature of the meniscus, and a buoyancy force associated with the wetted segments of the sphere and plate. When the effect of gravity is negligible, the buoyancy force too can be disregarded. The axial component of the surface-tension force (attractive if positive) acting on the sphere is

$$F_s = 2\pi R\sigma \sin\psi \sin(\theta_1 + \psi). \tag{15}$$

The capillary pressure force is

$$F_p = -2\pi H\sigma R^2 \sin^2\psi. \tag{16}$$

Hence, the total force on the sphere is

$$F_t = F_s + F_p = 2\pi\sigma R[\sin\psi \sin(\theta_1 + \psi) - HR\sin^2\psi]. \tag{17}$$

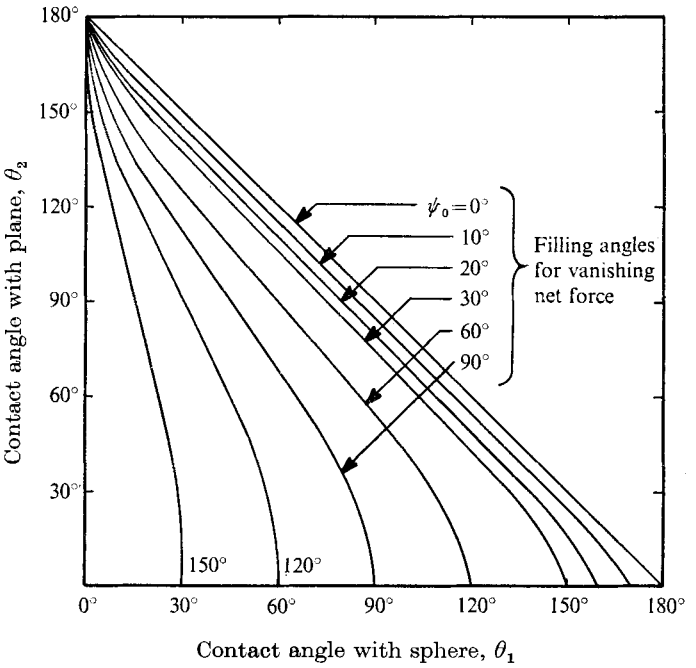

FIGURE 6. Filling angles for vanishing total force exerted by pendular ring (sphere on plate). Above the diagonal the force is always repulsive; below the diagonal the force is attractive if $\psi < \psi_0$, i.e. if the filling angle is less than the angle given by the curve through the point (θ_1, θ_2).

The force between a sphere and a plate has been measured by McFarlane & Tabor (1950) and that between a sphere and plane and between equal spheres by Cross & Picknett (1963*a*), Mason & Clark (1965*a*) and Erle *et al.* (1971). Cross & Picknett's data agree well with (13) when both surfaces are perfectly wetted by the liquid, i.e. when $\theta_1 = 0$ and $\theta_2 = 0$ (sphere on plate) and when $\theta_1 = 0$ and $\theta_2 = 90°$ (equal spheres). Their data for $\theta_1 = \theta_2 = 40°$ do not agree as well, which they attribute to difficulties in obtaining reproducible contact angles. Mason & Clark's data are not in good agreement with (17) but their measurements have been challenged by Erle *et al.* (1971), who confirm Cross & Picknett's results. McFarlane & Tabor (1950) reported measurements with spheres of different radii but did not record filling angles, which were probably quite small in most of their experiments.

In another paper Mason & Clark (1965*b*) showed that, when the total force between any two spheres is zero, the meniscus profile must be an arc of circle and the meniscus itself must be a zone of sphere. This is also true when the total force on a sphere in contact with a plane is zero. Because the principal radii of curvature of a spherical zone are equal, (17) dictates that when the separation is zero the filling angle ψ_0 at which the total force vanishes is given by

$$\tan(\tfrac{1}{2}\psi_0) = (\cos\theta_1 + \cos\theta_2)/\sin\theta_1. \tag{18}$$

Figure 6 is a working plot of this equation. It makes clear that if $\theta_1 = 0$ the zero-force configuration occurs only when $\psi_0 = 180°$. Apart from this limiting case

the total force is always attractive if the sphere is perfectly wetted by the liquid. However, if wetting is imperfect, i.e. θ_1 and θ_2 both different from zero, capillary attraction may give way to *capillary repulsion.*

The spherical configuration is important because it delimits the range of filling angles in which the total force on the sphere is attractive. If $\psi > \psi_0$, the total force is *repulsive*, a possibility that has been overlooked but which is certainly relevant to wetting and dispersion of pigments, adhesion of particles in moist atmospheres, and rheological behaviour of damp powders. The existence of capillary repulsion has recently been demonstrated by a simple experiment (Rivas *et al.* 1975). According to figure 6, if $\cos\theta_1 + \cos\theta_2 > 0$, ψ_0 is less than 180° and at larger filling angles the total force is repulsive. The zero-force filling angle ψ_0 can be quite small. For instance, if $\theta_2 = \frac{1}{2}\pi$, then $\psi_0 = \pi - 2\theta_1$; thus $\psi_0 = 10°$ when $\theta_1 = 85°$ and $\theta_2 = 90°$.

The azimuthal radius of meniscus curvature at the contact circle on the sphere is obviously

$$r_2 = R\sin\psi/\sin(\theta_1+\psi) \tag{19}$$

and therefore the mean curvature of the zero-force configuration is

$$HR = \sin(\theta_1+\psi_0)/\sin\psi_0.$$

With $\psi = \psi_0$ this matches the upper end of the range of mean curvatures of unduloids, as given by equation (11). The sphere is the transitional surface between unduloids and nodoids all of positive meridional curvature, just as the catenoid provides the transition between nodoids and unduloids all of negative meridional curvature.

Figures 5 and 6 are particularly useful because they define the ranges of filling angles in which most of the different formulae in table 1 apply.

Circle approximation

In the literature the meridional profile is often modelled by an arc of circle, which of course has uniform meridional curvature. Given θ_1, θ_2 and ψ the meridional radius is easily shown to be

$$r_1 = -\frac{R(1-\cos\psi)}{\cos(\theta_1+\psi)+\cos\theta_2}. \tag{20}$$

If this is used the second principal radius must also be taken as constant. A representative value which is convenient is the slant distance from the contact circle on the sphere to the axis of symmetry as given by equation (19)†. Together (19) and (20) provide an estimate $\tilde{H}$ of mean curvature:

$$2\tilde{H}R = -\frac{\cos(\theta_1+\psi)+\cos\theta_2}{1-\cos\psi} + \frac{\sin(\theta_1+\psi)}{\sin\psi}. \tag{21}$$

The circle approximation can also be used to estimate the total capillary force on the sphere or plane, and this has often been done for the limit of vanishing filling angle. Some trigonometric manipulation leads to

$$\tilde{F}_t = 2\pi\sigma R[\sin\psi\sin\theta_1 - (1+\cos\psi)(\cos\theta_1+\cos\theta_2)]. \tag{22}$$

† The azimuthal radius of curvature at any point of the circular arc could be used and would leave the estimates of meniscus area and enclosed volume unchanged, although it would give an estimate of mean curvature different from (21).

According to this equation the total force is independent of the amount of liquid in the ring as that amount approaches zero, inasmuch as

$$\lim_{\psi \to 0} \tilde{F}_t = 2\pi\sigma R(\cos\theta_1 + \cos\theta_2). \tag{23}$$

This is identical to the limit of the exact equation (17) and both predict that the limiting force is *repulsive* whenever wetting is sufficiently imperfect that

$$\theta_1 + \theta_2 > 180°.$$

This accords with (18) and figure 6. When $\theta_1 = \theta_2$, equation (23) reduces to formulae obtained by McFarlane & Tabor (1950) and Cross & Picknett (1963*a*); when $\theta_2 = 90°$, to a formula reported by Cross & Picknett (1963*a*).

The circle approximation is so much more tractable than the exact treatment of pendular rings that it is important to know when it is an accurate approximation. Now it is, in fact, the exact solution when the meniscus is actually spherical and therefore the mean curvatures, forces, volumes and surface areas from the approximation are exactly right when $\psi = \psi_0$. Unfortunately the accuracy of the approximation may deteriorate rapidly as ψ departs from ψ_0, particularly when θ_1 and θ_2 are both small. For instance, when $\theta_1 = \theta_2 = 40°$, $\psi_0 = 134{\cdot}48°$ and the errors $100(\tilde{H} - H)/|H|$ are 26·2 % and −47·5 % when $\psi = 130°$ and $\psi = 140°$, respectively.

The circle approximation is also the exact solution in the special limit of a cylindrical meniscus, i.e. when $\theta_1 + \psi = \theta_2 = 90°$.

It happens that the first term of (21) is the same as the first term of each formula in table 1. Consequently the circle approximation might be expected to be accurate when Ψ dominates the terms containing elliptic integrals in the table. This is true, at least when θ_1 and ψ are both small. Computations show that, for $\theta_1 \leqslant 60°$ and $\psi \leqslant 10°$, $\tilde{H}$ differs from H by less than 6·5 %. The estimate $\tilde{F}_t$ is slightly closer to F_t because the surface-tension part F_s can be computed exactly. The estimates of meniscus area and enclosed volume are accurate to within 5·5 % when $\theta_1 \leqslant 60°$ and $\psi \leqslant 40°$.

Effect of gravity

In order to assess the importance of gravity and to confirm the solutions obtained in § 2 we have also solved numerically the full Laplace–Young equation for axisymmetric menisci, which in dimensionless form is [cf. (1) and (2)]

$$By + 2H_0 R = \frac{d^2y/dx^2}{[1 + (dy/dx)^2]^{\frac{3}{2}}} + \frac{dy/dx}{x[1 + (dy/dx)^2]^{\frac{1}{2}}}, \tag{24}$$

where the Bond number is now $B \equiv gR^2\Delta\rho/\sigma$ and H_0 is the curvature at $y = 0$. Since y is of order one, the first term on the left side of (20) can be neglected when $B/|2HR| \ll 1$. Sample calculations were made with $B = 0{\cdot}014$ and several pairs of contact angles. In every case, the numerical and analytic solutions in no respect differ by more than 0·4 % (usually they are much closer) except when $2HR$ turns out to be sufficiently small that $B/|2HR| > 10^{-2}$. For instance, with sphere and plate in contact and $\theta_1 = \theta_2 = 40°$, the difference between $\tilde{H}$ and H

is only 0·19 % when $B/|2HR| = 0{\cdot}0132$; but when $B/|2HR| = 0{\cdot}210$, the difference is 7·6 %. It appears that the ratio of Bond number to dimensionless mean curvature provides a conservative criterion. If the Bond number is less than a specified small percentage of the product of mean curvature and sphere radius, the properties of the meniscus calculated by neglecting gravity evidently are in error by less than that percentage. Indeed, gravity may often be a less important perturbing influence than departures of contact lines from circularity and non-uniformities of contact angle along the contact lines, phenomena associated with rough and dirty solid surfaces and contaminated liquids.

This work was supported in part by the National Science Foundation. A. P. R. is grateful to the Latin American Scholarship Program of American Universities for its support.

Appendix. Stability of diffusional equilibrium states

The chemical potential of liquid in a pendular ring depends on the pressure within the ring and hence on the curvature of the ring surface, a fact which is expressed by an approximate relation named after Kelvin (e.g. Defay & Prigogine 1966),

$$\ln(P^0/P^{eq}) = v_L^0(p - P^{eq})/RT, \tag{25}$$

where R is the gas constant, T the absolute temperature, P^{eq} the pressure of vapour in equilibrium with liquid which itself experiences a pressure p, and P^0 the ordinary vapour pressure, i.e. the pressure of vapour in equilibrium with bulk liquid beneath a flat meniscus. v_L^0 is the molar volume of the liquid, the dependence of which on pressure is disregarded in deriving (25). For a system in mechanical equilibrium and vapour–liquid equilibrium,

$$p - P^{eq} = 2H\sigma. \tag{26}$$

Thus the Kelvin equation predicts that the vapour pressure of liquid behind a surface having negative mean curvature is lower than that of liquid at the same temperature beneath a surface of zero mean curvature. Hence vapour at the ordinary vapour pressure will condense into a pendular ring at the same temperature.

If the pressure in the vapour is less than the ordinary vapour pressure the equilibrium configuration of liquid is a ring having negative mean curvature given by equation (26). This configuration is stable since a small increase in the volume of liquid produces a driving force for volume decrease by evaporation, while a small decrease produces a driving force for volume increase by condensation.

If the pressure in the vapour exceeds the ordinary vapour pressure and no flat interfaces are in the vicinity, surfaces of positive mean curvature may exist in diffusional equilibrium. Depending on the pressure in the vapour there are as many as three different surfaces which have the same mean curvature. Figure 7 shows the possible equilibrium states. State 1 is stable: a small increase

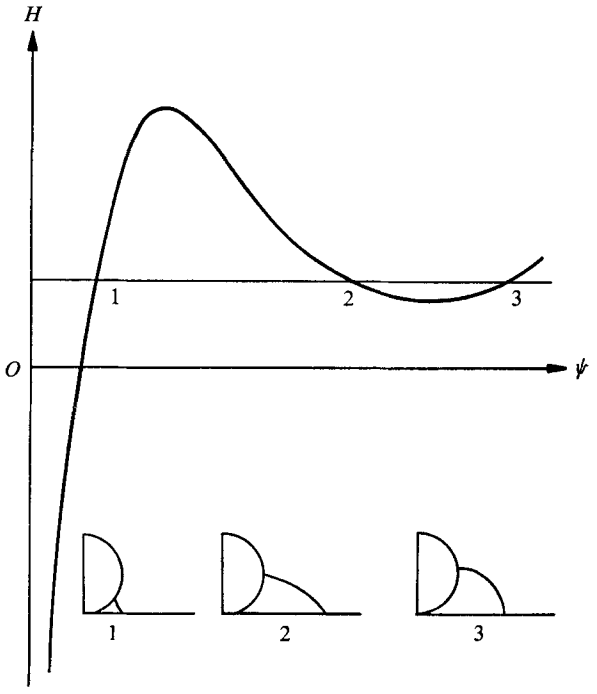

FIGURE 7. Mean curvature at equilibrium between ring liquid and vapour at a pressure exceeding the ordinary vapour pressure at the same temperature.

in the amount of liquid in the ring increases the filling angle and hence the curvature and so causes evaporation, while the converse is true of a small decrease in volume. State 2 is unstable because a small increase in its volume increases ψ, diminishes the mean curvature and promotes further condensation; similarly, a small decrease in volume decreases ψ, raises the mean curvature and enhances evaporation. State 3 is slightly different since increasing the volume *decreases* the filling angle, but this again diminishes the mean curvature and promotes condensation, while reducing the volume slightly leads to a tendency for further evaporation; hence this state is also unstable. It may also be susceptible to instability that depends on gravity, inasmuch as ψ would have to be comparatively large before state 3 became even a possibility.

REFERENCES

CARMAN, P. C. 1953 Properties of capillary held liquids. *J. Phys. Chem.* **57**, 56–68.

CLARK, W. C., HAYNES, J. M. & MASON, G. 1968 Liquid bridges between a sphere and a plane. *Chem. Engng Sci.* **23**, 810–812.

CROSS, N. L. & PICKNETT, R. G. 1963*a* Particle adhesion in the presence of a liquid film. In *The Mechanism of Corrosion by Fuel Impurities* (ed. H. R. Johnson & D. H. Littler), pp. 383–390. London: Butterworths.

CROSS, N. L. & PICKNETT, R. G. 1963*b* The liquid layer between spheres and a plane surface. *Trans. Faraday Soc.* **59**, 846–855.

DEFAY, R. & PRIGOGINE, I. 1966 In *Surface Tension and Absorption*, pp. 217–227. Wiley.

ERLE, M. A., DYSON, D. C. & MORROW, N. R. 1971 Liquid bridges between cylinders, in a torus, and between spheres. *A.I.Ch.E. J.* **17**, 115–121.

EVERETT, D. H. 1967 Adsorption hysteresis. In *The Solid–Gas Interface*, vol. 2 (ed. E. A. Flood), pp. 1055–1113. Dekker.

FISHER, R. A. 1926 On the capillary forces in an ideal soil; correction of formulae given by W. B. Haines. *J. Agric. Sci.* **16**, 492–505.

HAINES, W. B. 1925 A note on the cohesion developed by capillary forces in an ideal soil. *J. Agric. Sci.* **15**, 529–543.

HAINES, W. B. 1927 Studies in the physical properties of soils. *J. Agric. Sci.* **17**, 264–290.

HEADY, R. B. & CAHN, J. W. 1970 An analysis of the capillary forces in liquid-phase sintering of spherical particles. *Met. Trans.* **1**, 185–189.

HOWE, W. 1887 Rotations–Flächen welche bei vorgeschriebener Flächengrösse ein möglichst grosses oder kleines Volumen enthalten. Inaugural-Dissertation, Friedrich–Wilhelms–Universität zu Berlin.

KINGERY, W. D. 1959 Densification during sintering in the presence of a liquid phase. *J. Appl. Phys.* **30**, 301–306.

MCFARLANE, J. S. & TABOR, D. 1950 Adhesion of solids and the effect of surface films. *Proc. Roy. Soc.* A **202**, 224–243.

MASON, G. 1973 Formation of films from latices, a theoretical treatment. *Brit. Polymer J.* **5**, 101–108.

MASON, G. & CLARK, W. G. 1965*a* Liquid bridges between spheres. *Chem. Engng Sci.* **20**, 859–866.

MASON, G. & CLARK, W. C. 1965*b* Zero force liquid bridges between spherical particles. *Brit. Chem. Engng*, **10**, 327–328.

MAYER, R. P. & STOWE, R. A. 1966 Mercury porosimetry: filling of toroidal void volume following breakthrough between packed spheres. *J. Phys. Chem.* **70**, 3867–3873.

MELROSE, J. C. 1966 Model calculations for capillary condensation *A.I.Ch.E. J.* **12**, 986–994.

MELROSE, J. C. 1972 Chemical potential changes in capillary condensation. *J. Colloid Interface Sci.* **38**, 312–322.

MORROW, N. R. 1971 The retention of connate water in hydrocarbon reservoirs. *J. Can. Pet. Tech.* **10**, 38–46.

PLATEAU, J. 1864 The figures of equilibrium of a liquid mass. In *The Annual Report of the Smithsonian Institution*, pp. 338–369. Washington, D.C.

PUJADO, P. R., HUH, C. & SCRIVEN, L. E. 1972 On the attribution of an equation of capillarity to Young and Laplace. *J. Colloid Interface Sci.* **38**, 662–663.

RIVAS, A. P., ORR, F. M. & SCRIVEN, L. E. 1975 Capillary attraction–and capillary repulsion. *Latin Am. J. Chem. Engng. Appl. Chem.* **5** (in press).

ROSE, W. 1958 Volumes and surface areas of pendular rings. *J. Appl. Phys.* **29**, 687–691.

SHEETZ, D. P. 1965 Formation of films by drying of latex. *J. Polymer Sci.* **9**, 3759–3773.

VANDERHOFF, J. W., TARKOWSKI, H. L., JENKINS, M. C. & BRADFORD, E. B. 1966 Theoretical consideration of the interfacial forces involved in the coalescence of latex particles. *J. Macromolec. Chem.* **1**, 361–397.

WOODROW, J., CHILTON, H. & HAWES, R. I. 1961 Forces between slurry particles due to surface tension. *J. Nucl. Energy* B, *Reactor Tech.* **2**, 229–237.

ZIMON, A. D. 1969 *Adhesion of Dust and Powder*. Plenum.